EphA2 Immunoconjugate as Molecularly Targeted Chemotherapy for Ovarian Carcinoma

Jeong-Won Lee, Hee Dong Han, Mian M. K. Shahzad, Seung Wook Kim, Lingegowda S. Mangala, Alpa M. Nick, Chunhua Lu, Robert R. Langley, Rosemarie Schmandt, Hye-Sun Kim, Shenlan Mao, John Gooya, Christine Fazenbaker, Dowdy Jackson, David A. Tice, Charles N. Landen, Robert L. Coleman, Anil K. Sood

Background   EphA2 is overexpressed in many types of human cancer but is absent or expressed at low levels in normal epithelial tissues. We investigated whether a novel immunoconjugate containing an anti-EphA2 monoclonal antibody (1C1) linked to a chemotherapeutic agent (monomethyl auristatin phenylalanine [MMAF]) through a noncleavable linker maleimidocaproyl (mc) had antitumor activity against ovarian cancer cell lines and tumor models.

Methods   Specificity of 1C1-mcMMAF was examined in EphA2-positive HeyA8 and EphA2-negative SKMel28 ovarian cancer cells by antibody binding and internalization assays. Controls were phosphate-buffered saline (PBS), 1C1, or control IgG-mcMMAF. Viability and apoptosis were investigated in ovarian cancer cell lines and tumor models (10 mice per group). Antitumor activities were tested in the HeyA8-luc and SKOV3ip1 orthotopic mouse models of ovarian cancer. Endothelial cells were identified by use of immunohistochemistry and anti-CD31 antibodies. All statistical tests were two-sided.

Results   The 1C1-mcMMAF immunoconjugate specifically bound to EphA2-positive HeyA8 cells but not to EphA2-negative cells and was internalized by HeyA8 cells. Treatment with 1C1-mcMMAF decreased the viability of HeyA8-luc cells in an EphA2-specific manner. In orthotopic mouse models, treatment with 1C1-mcMMAF inhibited tumor growth by 85%–98% compared with that in control mice (eg, for weight of HeyA8 tumors, 1C1-mcMMAF = 0.05 g and control = 1.03 g; difference = 0.98 g, 95% confidence interval [CI] = 0.40 to 1.58 g; P = .001). Even in bulkier disease models with HeyA8-luc cells, 1C1-mcMMAF treatment, compared with control treatment, caused regression of established tumors and increased survival of the mice (eg, 1C1-mcMMAF vs control, mean = 60.6 days vs 29.4 days; difference = 31.2 days, 95% CI = 27.6 to 31.2 days; P = .001). The antitumor effects of 1C1-mcMMAF therapy, in SKOV3ip1 tumors, for example, were statistically significantly related to decreased proliferation (eg, 1C1-mcMMAF vs control, mean = 44.1% vs 55.8% proliferating cells; difference = 11.7%, 95% CI = 2.45% to 20.9%; P = .01) and increased apoptosis of tumor cells (eg, 1C1-mcMMAF vs control, mean = 8.6% vs 0.9% apoptotic cells; difference = 7.7%, 95% CI = 3.8% to 11.7%; P < .001) and of mouse endothelial cells (eg, 1C1-mcMMAF vs control, mean 2.8% vs 0.4% apoptotic endothelial cells; difference = 2.4%, 95% CI = 1.4% to 4.6%; P = .034).

Conclusion   The 1C1-mcMMAF immunoconjugate had antitumor activity in preclinical models of ovarian carcinoma.

J Natl Cancer Inst 2009;101:1193–1205

Ovarian cancer is the most common cause of death from a gynecologic malignancy (1). Although most patients with advanced-stage ovarian cancer will die of the disease, more than 70% have a favorable initial response to surgery and chemotherapy and a substantial fraction will respond to second-line therapies (2,3). Systemic chemotherapy is widely used but is frequently associated with intolerable side effects (4). Given the high mortality rate of ovarian cancer, new therapies are urgently needed to target the tumor while sparing normal tissues.

Affiliations of authors: Department of Gynecologic Oncology (J-WL, HDH, MMKS, SWK, LSM, AMN, CL, RS, H-SK, CNL, RLC, AKS) and Department of Cancer Biology (RRL, AKS), University of Texas M.D. Anderson Cancer Center, Houston, TX; Department of Obstetrics and Gynecology, Samsung Medical Center, Sungkyunkwan University School of Medicine, Seoul, Korea (J-WL); Department of Obstetrics and Gynecology, Baylor College of Medicine, Houston, TX (MMKS); Department of Pathology, Cheil General Hospital and Women's Healthcare Center, Kwandong University College of Medicine, Seoul, Korea (H-SK); MedImmune, Gaithersburg, MD (SM, JG, CF, DJ, DAT).

Correspondence to: Anil K. Sood, MD, Department of Gynecologic Oncology and Department of Cancer Biology, The University of Texas M.D. Anderson Cancer Center, 1155 Herman Pressler, Unit 1352, Houston, TX 77030 (e-mail: asood@mdanderson.org).

See "Funding" and "Notes" following "References."

CONTEXT AND CAVEATS

Prior knowledge
EphA2 is a receptor tyrosine kinase that is overexpressed in many human cancers but is absent or expressed at low levels in normal epithelial tissues.

Study design
The antitumor activity of an immunoconjugate containing an anti-EphA2 monoclonal antibody (1C1) linked to a chemotherapeutic agent (monomethyl auristatin phenylalanine [MMAF]) through a noncleavable linker maleimidocaproyl (mc) was studied in ovarian cancer cell lines and ovarian tumor models in mice.

Contribution
The 1C1-mcMMAF immunoconjugate had antitumor activity in ovarian cancer cell lines and preclinical models of ovarian cancer.

Implications
Additional preclinical investigations into the antitumor activity of 1C1-mcMMAF and its safety are warranted.

Limitations
The activity of 1C1-mcMMAF that has actually been delivered into a solid tumor mass has not been studied. Unexpected toxicities in future research cannot be ruled out, especially to EphA2-expressing normal tissues or cells. Analyses in this study were done in cultured cell lines and in mouse models that used immunodeficient mice, and so results may not necessarily translate into human patients with ovarian cancer.

From the Editors

Monoclonal antibodies may be a potential type of new therapy. Human and chimeric monoclonal antibodies (including bevacizumab, rituximab, trastuzumab, alemtuzumab, and cetuximab) have been shown to be highly selective therapeutic agents for cancer (5). Immunoconjugates containing a monoclonal antibody and a chemotherapeutic agent provide another approach to selectively deliver toxins or cytotoxic agents to various types of cancer, including gemtuzumab ozogamicin, ^{90}Y-labeled ibritumomab tiuxetan, and ^{131}I-labeled tositumomab (6). An ideal target for such an immunoconjugate would be a molecule that is expressed at much higher levels in the tumor than in normal tissues or expressed in tumor tissue but not in normal tissue. Such a target may be the EphA2 receptor, which is overexpressed by many human cancers including ovarian, lung, prostate, colorectal, melanoma, and brain malignancies but is expressed at low levels in only some normal epithelial tissues including kidney, lung, colon, and bladder (7–10). EphA2 overexpression has been associated with poor prognosis in patients with ovarian, esophageal, and renal cancers. It is thought that EphA2 overexpression leads to mislocalization and loss of contact with the ephrin ligands, leading to an increase in adhesions between cells and the extracellular matrix and higher invasive potential (10). It has been shown (11) that stimulation of the unbound EphA2 receptor with soluble ephrin ligand inactivates Ras and reduces phosphorylation of focal adhesion kinase and extracellular signal-regulated kinase in some model systems.

The purpose of this study was to investigate the antitumor activity of the 1C1-mcMMAF immunoconjugate in ovarian cancer

cell lines and three orthotopic mouse models of ovarian carcinoma. For this analysis, we used a fully human anti-EphA2 monoclonal antibody (1C1), which has been shown to bind selectively to the extracellular domains of the human and mouse EphA2 receptor (11). For the chemotherapeutic agent, we used derivatives of auristatin, which inhibits polymerization of microtubules. Auristatins have been used as potent cytotoxic agents in human breast, lymphoma, and colorectal cells and have been delivered to tumors, including lung adenocarcinoma and lymphoma, by conjugated antibodies (12). Two modified auristatins, monomethyl auristatin E (which is cell permeable) and monomethyl auristatin phenylalanine (MMAF, which is cell impermeable), have been conjugated to antibodies through various linkers (13). Although auristatins are fairly inactive when not conjugated to an antibody, their potency has been shown to increase by approximately three orders of magnitude after conjugation with the cAC10 antibody against CD30 (13). The EphA2 immunoconjugate, 1C1-mcMMAF, was formed by conjugating a monoclonal antibody against EphA2 (1C1) with MMAF through a noncleavable linker maleimidocaproyl (mc) linker (11).

Materials and Methods

Antibodies and Immunoconjugates

1C1 (fully human monoclonal antibody recognizing both human and murine EphA2), IgG-mcMMAF (nonspecific IgG monoclonal antibody conjugated to MMAF via the mc linker), and 1C1-mcMMAF (1C1 conjugated to MMAF via the mc linker) were used in this study (11). All of these monoclonal antibodies and their conjugates were kind gifts from MedImmune (Gaithersburg, MD). The antibody description and the details of the conjugation reaction have been described previously (11). To evaluate the level of EphA2 after treatment of antibodies, we used anti-EphA2 (clone 1C11A12; Zymed, Camarillo, CA) or anti–glyceraldehyde-3-phosphate dehydrogenase monoclonal antibody (Applied Biosystems, Foster City, CA) for Western blot analysis and immunohistochemistry.

Cell Lines and Culture Conditions

Sources of the human epithelial ovarian cancer cell lines that were used in this study—HeyA8 cell line, luciferase-transfected HeyA8 cells (HeyA8-luc) cell line, the SKOV3ip1 cell line, the taxane-resistant HeyA8-MDR cell line, and mouse ovarian endothelial cells—have been described previously (14–16). Briefly, HeyA8, HeyA8-luc, and SKOV3ip1 cells were maintained in RPMI 1640 medium supplemented with 15% fetal bovine serum and 0.1% gentamycin sulfate (Gemini Bioproducts, Calabasas, CA) (14–16). The HeyA8-MDR cell line, a taxane-resistant line that was generated by sequential exposure to increasing concentrations of paclitaxel (Bristol-Myers Squibb, New York, NY), was maintained in the above medium with paclitaxel at 300 µg/mL. Mouse ovarian endothelial cells that were isolated from an ovary of the ImmortoMice whose tissues harbor a temperature-sensitive simian virus 40 large tumor (T) antigen (ie, *H-2K^b-tsA58* mice) (17) were maintained in Dulbecco's modified Eagle medium with 10% fetal bovine

serum. In addition, we used several human ovarian cancer cell lines including SKOV3-luc, SKOV3-TR, A2780-par, A2780-CP20, OVCAR, IGROV, and 222 to evaluate the baseline expression levels of EphA2. All of these cell lines are of human background, and sources have been described previously (18). The SKMel28 human melanoma cells were maintained in a 5% CO_2 humidified incubator as monolayer cultures in RPMI 1640 supplemented with 10% Nu-Serum (Collaborative Research Products, Bedford, MA), 1 mM aminoguanidine, penicillin (50 Units/mL), and streptomycin (50 µg/mL) (19). All cultures were used when cells were 70%–80% confluent.

Europium-Labeled Antibody-Binding Assays to Cell Surface EphA2

For both assays, 1C1-mcMMAF immunoconjugates, 1C1 monoclonal antibodies, and isotype controls (IgG and IgG-mcMMAF) were labeled with europium according to the manufacturer's instructions (PerkinElmer, Waltham, MA). Briefly, for cell-binding assays, exponentially proliferating HeyA8 and SKMel28 cells were detached from their culture dishes with cell dissociation solution (Invitrogen, Eugene, OR) and suspended in ice-cold binding buffer containing 50% of DELFIA L*R binding buffer (PerkinElmer) and 50% of stabilizer, and 5×10^4 cells were added to each well of 96-well plates, followed by 200 μL of binding buffer containing 2 nM europium-labeled 1C1, 2 nM europium-labeled 1C1-mcMMAF, 2 nM europium-labeled IgG, or 2 nM europium-labeled IgG-mcMMAF. The plates were incubated for 1 hour at 4°C. Binding was terminated by four washes with ice-cold DELFIA L*R wash buffer (PerkinElmer). A total of 200 µL of enhancement solution was added per well, and plates were then shaken for 15 minutes at room temperature and then read with a Wallac Victor instrument that measures europium via time-resolved fluorescence.

For the recombinant EphA2-binding assay, wells of 96-well plates were coated with the extracellular domain of recombinant human EphA2 (5 µg/mL), of recombinant mouse EphA2 (2 µg/mL), of recombinant rat EphA2 extracellular domain (10 µg/mL), or of recombinant cynomolgus monkey EphA2 (5 µg/mL) in 25 µL of 100 mM sodium carbonate buffer (pH 9.4) at 4°C overnight. The plates were washed once with DELFIA assay buffer (PerkinElmer) and incubated with blocking buffer containing 50% DELFIA assay buffer and 50% stabilizer (PerkinElmer) for 1 hour at room temperature. Europium-labeled 1C1-mcMMAF or 1C1 were diluted in blocking buffer to various concentrations from 0.01 to 10 nM, and then, 25 µL of each dilution was added to two wells. Nonspecific binding was assessed by using a mixture of unlabeled to labeled antibody or immunoconjugate at a 100:1 ratio, and then, 25 µL of each dilution was added to two wells. After a 2-hour incubation at room temperature, the plates were washed four times with DELFIA wash buffer, 100 µL of enhancement solution (PerkinElmer) was added to each well, and plates were shaken for 15 minutes at room temperature and then read as described above. The equilibrium dissociation constant for europium-labeled 1C1 and for europium-labeled 1C1-mcMMAF was calculated by analyzing saturation binding curves with the one-site-fit program of GraphPad Prism software (La Jolla, CA).

Antibody Internalization Assay

Adherent HeyA8 and SKMel28 cells in logarithmic growth phase were removed from culture flasks with GIBCO cell dissociation buffer (Invitrogen), placed in growth medium, and then, 100 µL containing 0.5×10^6 viable HeyA8 cells was placed in each well of a 96-well U-bottomed plate. Plates were centrifuged at 500g for 5 minutes to pellet cells. Buffer was removed by aspiration, and cells were resuspended in 100 µL of phosphate-buffered saline (PBS) containing the 1C1-mcMMAF immunoconjugate or the isotype control immunoconjugate IgG-mcMMAF (each at 5 µg) and then incubated for 30 minutes at 4°C. Cells were washed twice with PBS to remove unbound immunoconjugate. Cells were allowed to internalize the immunoconjugates that were bound to their surface by resuspending cells in 100 µL of growth medium and incubating them for 30 minutes at 37°C in an atmosphere of 5% CO_2 and 95% air. As a negative control, cells were incubated on ice for 30 minutes. Cells were then fixed in 4% paraformaldehyde in PBS for 20 minutes at room temperature and permeabilized in 0.5% Triton X-100 in PBS for 5 minutes at room temperature. Cells were incubated with 1 µg of AlexaFluor 488–labeled goat anti-human IgG antibody (Biosource, Camarillo, CA) in 100 µL of PBS containing 2% fetal bovine serum for 30 minutes at 4°C. Cells were washed twice with ice-cold PBS between each step above and then resuspended in 200 µL of PBS and centrifuged onto coated slides by use of Shandon EZ Single Cytofunnels and Shandon Cytospin 3 at 101.5g for 7 minutes at room temperature. Finally, the cells were covered with VECTASHIELD hardset mounting medium containing 4′,6-diamidino-2-phenylindole (Vector Laboratories, Burlingame, CA) and a coverslip before qualitative examination and photography with fluorescent microscope.

Western Blot Analysis of EphA2 Protein in Ovarian Cancer Cell Lysates and Tumors

Preparation of lysates from cultured cells and tumors has been described previously (8,15). EphA2 expression was evaluated in untreated cultured HeyA8 and SKOV3ip1 ovarian cancer cells and mouse ovarian endothelial cells and in cells that had been treated with 1C1, IgG-mcMMAF, or 1C1-mcMMAF (each at 100 ng/mL) for 24, 48, or 72 hours. Briefly, lysates of cultured cells were prepared by washing cells with PBS and then incubating them in modified RIPA lysis buffer (50 mM Tris, 150 mM NaCl, 1% Triton X-100, and 0.5% deoxycholate) containing leupeptin at 25 µg/mL, aprotinin at 10 µg/mL, 2 mM EDTA, and 1 mM sodium orthovanadate (Sigma, St. Louis, MO) for 10 minutes at 4°C. Lysed cells were removed from plates by scraping and then centrifuging at 11 000g for 20 minutes at 4°C, and the supernatant was stored at −80°C. Each experiment was performed three times.

To evaluate EphA2 expression in HeyA8-luc tumors after immunoconjugate treatment, mice were injected with HeyA8-luc cells and then 17 days later (when palpable intraperitoneal tumors were detected) were injected intraperitoneally once with 1C1-mcMMAF at 3 mg/kg or with PBS as control. Mice were killed at 1, 3, 5, or 10 days, and tumors were excised, immediately snap-frozen in liquid nitrogen, and stored at −80°C. A portion of the tissue (50–100 mm³) that was confirmed (by staining with

hematoxylin–eosin) to contain tumor was incubated on ice in RIPA lysis buffer containing protease inhibitors (leupeptin at 25 μg/mL and aprotinin at 10 μg/mL) for 2 hours, homogenized with a mortar and pestle, and processed as described above for cells.

For both cell and tumor lysates, protein concentrations were determined with a BCA Protein Assay Reagent kit (Pierce Biotechnology, Rockford, IL), and 20 μg of lysate protein per lane was subjected to sodium dodecyl sulfate–polyacrylamide gel electrophoresis on 10% gels. Protein bands were transferred to membranes and subjected to Western blot analysis for EphA2, as described previously (20). Briefly, the membranes were incubated overnight at 4°C with a primary monoclonal antibody that recognizes both mouse and human EphA2 (clone D7; Upstate, Lake Placid, NY) by following the manufacturer's recommendations. Antibody binding was detected by incubating blots with horseradish peroxidase (HRP)–conjugated horse anti-mouse IgG or horse anti-rabbit IgG (Amersham, Piscataway, NJ; each at 1 μg/mL). HRP was visualized by use of an enhanced chemiluminescence detection kit (Pierce Biotechnology). Equal loading and transfer were confirmed by probing the blots for β-actin (with anti–β-actin primary antibody at 0.1 μg/mL; Sigma).

Cytotoxicity Assay for HeyA8-luc Ovarian Cancer Cells

Cytotoxicity of 1C1-mcMMAF, 1C1, and IgG-mcMMAF treatments in HeyA8-luc cells was determined by use of the 3-(4,5-dimethylthiazol-2-yl)-2,5-diphenyltetrazolium bromide (MTT) uptake assay, as described previously (19). Briefly, 2×10^3 HeyA8-luc cells with RPMI 1640 medium supplemented with 15% fetal bovine serum and 0.1% gentamycin sulfate were plated in each well of a 96-well plate. Twenty-four hours after plating, the medium was replaced with 200 μL of fresh medium. At various times after antibody exposure, growth was assessed by adding 50 μL of 0.15% MTT (Sigma) to each well. After incubation for 2 hours at 37°C, medium was removed from the well and 100 μL of dimethyl sulfoxide was added (Sigma). The plate was shaken briefly to mix the samples, and the absorbance at 570 nm was recorded by using a Falcon microplate reader (Becton Dickinson Labware, Franklin Lakes, NJ). Each sample at each condition was assayed in triplicate.

Apoptosis Assays in Ovarian Cancer Cell Lines

Apoptosis was assessed by cell morphology and by use of an Annexin V–coupled fluorescein isothiocyanate (FITC) apoptosis detection kit-1 (BD Pharmingen, San Diego, CA). EphA2-positive HeyA8-luc cells were incubated for 48 or 72 hours alone (control) or with anti-EphA2 monoclonal antibody 1C1, the control immunoconjugate IgG-mcMMAF, or the immunoconjugate 1C1-mcMMAF (each at 100 ng/mL). Cell morphology was assessed by phase-contrast microscopy.

For the Annexin V–coupled FITC assay of apoptosis, the relative percentage of apoptotic HeyA8-luc and SKOV3ip1 cells was assessed at 24, 48, or 72 hours after treatment with 1C1, IgG-mcMMAF, or 1C1-mcMMAF (each at 100 ng/mL). Briefly, cells were removed from a six-well plate by incubation with trypsin–EDTA, washed twice in PBS, and resuspended in 1 mL of Annexin V–binding buffer at 10^6 cells per milliliter. Annexin V–coupled

FITC and propidium iodide (a probe to distinguish viable from nonviable cells) were added (each at 5 μL per 10^5 cells). Samples were mixed gently, incubated for 15 minutes at room temperature in the dark, and then subjected to flow cytometry analysis for apoptosis. Viable cells with intact membranes exclude propidium iodide, whereas the membranes of dead and damaged cells are permeable to propidium iodide. Cells that stain positive for Annexin V–coupled FITC and negative for propidium iodide are identified as undergoing apoptosis. Cells that stain positive for both Annexin V–coupled FITC and propidium iodide are in the late stage of apoptosis, are undergoing necrosis, or are already dead. Cells that stain negative for both Annexin V–coupled FITC and propidium iodide are alive and not undergoing measurable apoptosis.

Orthotopic Implantation of Tumor Cells in Mice

Female athymic mice (NCr-nu) were purchased from the National Cancer Institute–Frederick Cancer Research and Development Center. The mice were housed and maintained under specific pathogen-free conditions in facilities approved by the American Association for Accreditation of Laboratory Animal Care and in accordance with the current regulations and standards of the US Department of Agriculture, the US Department of Health and Human Services, and the National Institutes of Health. All studies were approved and supervised by the University of Texas M. D. Anderson Cancer Center Institutional Animal Care and Use Committee. The mice used in these experiments were 8–12 weeks old. To produce tumors, mice (n = 10 per group) were injected intraperitoneally with 1×10^6 SKOV3ip1 or HeyA8-MDR cells in 0.2 mL of Hanks balanced saline solution (HBSS; Life Technologies Invitrogen, Carlsbad, CA) or 2.5×10^5 HeyA8-luc cells in 0.2 mL of HBSS. The number of tumors was variable (usually 1–25 nodules in HeyA8-luc, 1–26 nodules in SKOV3ip1, and 1–18 nodules in HeyA8-MDR model). Most of the tumors were located in the omentum, pelvis, peritoneum, mesentery, bowel wall, porta hepatis, diaphragm, or around the spleen. Mice were monitored daily for adverse effects of therapy (eg, weight loss, decreased activity, and decreased food or water intake) and were killed by cervical dislocation on day 35 (SKOV3ip1) or day 28 (HeyA8-luc or HeyA8-MDR) after tumor cell injection or when any of the mice appeared moribund. Total body weight, ascites, tumor weight, locations, and the number of tumor nodules in the abdomen were recorded. The tumor weight from each mouse was determined by weighing all of the tumor nodules together. Tumors were fixed in formalin and embedded in paraffin or were snap-frozen in optimal cutting temperature (OCT) compound (Sakura Finetek USA, Inc, Torrance, CA) in liquid nitrogen.

Immunoconjugate Treatment of Established Tumors in Nude Mice

Before investigating whether EphA2 immunoconjugates have antitumor activity in our mouse model, we performed preliminary time–response experiments for 1C1-mcMMAF. Seventeen days after HeyA8-luc cell inoculation (when tumors were palpable), mice were injected intraperitoneally once with PBS (as a control) or with 1C1-mcMMAF at 3 mg/kg. Randomly selected mice from

each group were killed on days 1, 3, 5, or 10 after treatment (n = 3 on each day), and tumors were collected for Western blot and immunohistochemistry analyses to determine the level of EphA2 expression.

To investigate the antitumor activity of the immunoconjugate, 1.0×10^6 SKOV3ip1 cells or 2.5×10^5 HeyA8-luc cells were injected once intraperitoneally into mice and therapy was initiated 7 days later with PBS (200 μL) or with 1C1, IgG-mcMMAF, or 1C1-mcMMAF (each at 3 mg/kg in 200 μL of PBS). Weekly intraperitoneal injections were given until mice in any group became moribund. To evaluate the antitumor activity of the immunoconjugates against taxane-resistant tumors, the HeyA8-MDR model was used. Briefly, 1.0×10^6 HeyA8-MDR cells were injected intraperitoneally into mice, and therapy was initiated 7 days later as described above, except that another treatment group that received docetaxel (Sanofi-Aventis, Bridgewater, NJ) was included and the IgG-mcMMAF treatment was not included. Weekly intraperitoneal injections were continued until mice in any group became moribund.

Bioluminescence Imaging of Tumors in Tumor-Bearing Mice

Mice were injected intraperitoneally with 2.5×10^5 HeyA8-luc cells per mouse (n = 5 mice per group). After 17 days, mice were randomly picked out of the entire pool once a week until the first mouse became moribund and assigned to one of four treatment groups: control (200 μL of PBS) or 1C1, IgG-mcMMAF, or 1C1-mcMMAF (each at 3 mg/kg in 200 μL of PBS). For longitudinal assessment, bioluminescence imaging was conducted at 17, 23, 25, 27, and 31 days after tumor cell injection. Bioluminescence imaging and data acquisition with the IVIS 100 imaging system coupled to the Living Image software (Xenogen, Alameda, CA) were done twice a week, as reported previously (14). Briefly, mice were anesthetized in an acrylic chamber with a mixture of 1.5% isoflurane in air and injected intraperitoneally with luciferin potassium salt (15 mg/mL) in PBS at a dosage of 150 mg/kg of body weight. A digital gray-scale animal image was acquired followed by acquisition and overlay of a pseudocolor image representing the spatial distribution of detected photons emerging from active luciferase within the animal. Signal intensity was expressed as the sum of all detected photons per second within the abdominal cavity where tumor cells were injected.

Immunohistochemistry of EphA2 and Proliferating Cell Nuclear Antigen (PCNA) in HeyA8-luc Tumors

Immunohistochemical analysis of EphA2 and PCNA to identify proliferating tumor cells was conducted on established tumors with HeyA8-luc cells that were excised from mice. EphA2 staining was performed with the tissue samples used in the time–response experiment with 1C1-mcMMAF, and PCNA staining was performed with the tissue samples used in immunoconjugate therapy experiments. The immunohistochemistry was performed as described previously (8,21). Briefly, formalin-fixed paraffin-embedded tissue samples were cut into 8-μm sections and washed sequentially in xylene, 100% ethanol, 95% ethanol, 80% ethanol, and PBS. Antigen retrieval was then performed by heating slides

in a steam cooker for 10 minutes in 0.2 M Tris buffer at pH 9.0 (for EphA2) or in a microwave for 5 minutes in 0.1 M sodium citrate buffer at pH 6.0 (for PCNA). After two washes in PBS, slides were blocked with 5% normal horse serum and 1% normal goat serum in PBS (blocking solution) for 15 minutes at room temperature and then incubated with primary antibody against PCNA (PC-10, mouse IgG; DakoCytomation, Carpinteria, CA) in blocking solution overnight at 4°C. After two washes with PBS, the appropriate HRP-conjugated secondary antibody in blocking solution was added for 1 hour at room temperature. Slides were stained with diaminobenzidine substrate (Phoenix Biotechnologies, Huntsville, AL) for 5 minutes, washed, and counterstained with Gill No. 3 hematoxylin (Sigma) for 20 seconds. For the analysis of EphA2, after the slides were treated to block endogenous peroxidase activity, they were incubated with mouse IgG Fc blocker (Jackson Laboratory, Bar Harbor, ME; 0.13 μg/mL) for 2 hours before incubation with the primary antibody (EA5 clone; MedImmune). For EphA2 staining, 0.5% blocking reagent was used (from the TSA Biotin System kit; PerkinElmer Applied Biosystems, Boston, MA), and to visualize antibody binding, it was necessary to enhance the signal by treating slides with biotinylated horse anti-mouse antibody (Vector Laboratories; 1.5 μg/mL) for 10 minutes at room temperature, followed by streptavidin–HRP (DakoCytomation; 0.75 μg/mL) for 30 minutes. After a PBS wash, diaminobenzidine was added for 7 minutes and slides were counterstained with hematoxylin and mounted under coverslips.

Immunofluorescence Staining for CD31 and Terminal Deoxynucleotidyltransferase-Mediated Nick End Labeling (TUNEL) in Ovarian Tumors From Mice

Established tumors from mice treated with the immunoconjugate (3 mg/kg once per week) were excised, placed immediately in OCT compound, and frozen rapidly in liquid nitrogen. Frozen tissues were used for immunofluorescence staining for CD31 and TUNEL as described previously (22). Briefly, sections were fixed in acetone for 5 minutes, in a 1:1 mixture of acetone and chloroform (vol/vol) for 5 minutes, and then in acetone for 5 minutes. They were then washed with PBS, blocked with 10% fish gelatin in PBS for 20 minutes, and exposed to rat anti-CD31 antibody (platelet endothelial cell adhesion molecule-1, rat IgG, Pharmingen, San Jose, CA; 1:400 dilution) in blocking solution for 18 hours at 4°C, followed by anti-rat secondary antibody coupled to Texas Red (Molecular Probes, Eugene, OR; 1:200 dilution). Slides were washed in PBS, fixed again in 4% paraformaldehyde in PBS, washed twice in PBS, and incubated with 0.2% Triton X-100 in PBS for 15 minutes. After two more washes in PBS, slides were incubated for 10 minutes with the equilibration buffer in the TUNEL detection kit (Promega, Madison, WI). Equilibration buffer was removed, and reaction buffer (consisting of equilibration buffer in the kit, fluorescein-12-dUTP [where dUTP is deoxyribouridine triphosphate], and terminal deoxynucleotidyltransferase) was then added. After 1-hour incubation at 37°C in the dark, the reaction was stopped by addition of the provided 2× standard saline-buffered citrate (8.77 g of NaCl, 4.41 g of sodium citrate, and 400 mL of deionized water) for 15 minutes. Excess dUTP was removed by washing, and nuclei were stained with

Hoechst (Molecular Probes, in PBS; 1.0 μg/mL) for 10 minutes. Slides were covered with propylgallate and coverslips for microscopic evaluation. Microscopy was performed with a Zeiss AxioPlan 2 microscope, Hamamatsu ORCA-ER digital camera, and ImagePro software. The total number of CD31-positive cells (red staining) and apoptotic CD31-positive cells (red cells plus green nuclei) were counted. Controls included exposure to only secondary antibodies, exposure to reaction buffer that did not contain terminal deoxynucleotidyltransferase, and exposure to DNase to fragment the DNA (positive control). Apoptotic endothelial cells were counted in 10 random microscopic fields from each tumor (one slide per mouse, five slides per group) at ×200 magnification by two investigators in blinded fashion. The results were calculated, and the data are presented as the mean and 95% confidence interval (CI).

Statistical Analysis

Continuous variables were compared with the two-sample t test (between two groups) or with analysis of variance (ANOVA; for all groups) if normally distributed (as determined by the Kolmogrov–Smirnov test), and the Mann–Whitney test was used if distributions were nonparametric. For in vivo therapy experiments, 10 mice were randomly assigned to each treatment group. This sample size gave 80% power to detect a 50% reduction in tumor weight at a 5% level of statistical significance. ANOVA for tumor weight and the logarithm of tumor weight were used to examine interactions between treatments. Survival curves were plotted by the Kaplan–Meier method and tested for differences with the log-rank statistic. A P value of less than .05 from a two-tailed statistical test was considered statistically significant. All statistical tests were two-sided.

Results

Antibody Binding, Internalization, and Degradation Assay of EphA2 Immunoconjugates

The immunoconjugate was assembled by use of monoclonal antibody 1C1 against EphA2, a noncleavable linker maleimidocaproyl (mc) to couple the antibody to the chemotherapeutic agent, and a chemotherapeutic agent, monomethyl auristatin phenylalanine (MMAF). Immunofluorescence studies showed both 1C1 monoclonal antibodies and 1C1-mcMMAF immunoconjugates specifically bound to EphA2-positive HeyA8 cells, but neither bound to EphA2-negative SKMel28 cells. The binding affinities (as assessed by the dissociation constant) of europium-labeled 1C1 and 1C1-mcMMAF to cell surface EphA2 were evaluated and found to range from 0.98 to 1.52 nM across human, rat, and cynomolgus monkey EphA2. The binding affinities of 1C1 and 1C1-mcMMAF for recombinant mouse, human, rat and cynomolgus monkey EphA2 ranged from 0.43 to 0.96 nM. For human EphA2, the dissociation constants were 0.43 nM (95% CI = 0.38 to 0.48 nM) for 1C1 and 0.59 nM (95% CI = 0.48 to 0.70 nM) for 1C1-mcMMAF. Thus, the addition of the linker and chemotherapeutic agent (ie, mcMMAF) did not reduce the binding affinity of the monoclonal antibody 1C1 for recombinant EphA2 and native EphA2 expressed on cell surface (Figure 1, A). The ability of HeyA8 cells to internalize the immunoconjugate 1C1-mcMMAF was shown by immunofluorescence (Figure 1, B). In

addition, incubation of HeyA8 cells with 1C1 monoclonal antibodies or 1C1-mcMMAF immunoconjugate decreased EphA2 levels in a time-dependent manner, whereas incubation with control IgG or IgG-mcMMAF did not (Figure 1, C). These results indicate that the 1C1 antibody has agonist properties, with the treatment of cells with 1C1 leading to EphA2 degradation (8).

Sensitivity of Ovarian Cancer Cell Lines to 1C1-mcMMAF Immunoconjugates

We first examined apoptosis as assessed by cell morphology by phase-contrast microscopy. EphA2-positive HeyA8-luc cells were incubated for 48 or 72 hours alone (control) or with the anti-EphA2 monoclonal antibody 1C1, the control immunoconjugate IgG-mcMMAF, or the immunoconjugate 1C1-mcMMAF (each at 100 ng/mL). Apoptotic cells displayed cell shrinkage, a rounded morphology, and increased detachment (Figure 2, A). More apoptotic cells were found in cultures treated with 1C1-mcMMAF for 48 or 72 hours than in control (no treatment) cultures or in those treated with 1C1 or IgG-mcMMAF. We tested the cytotoxicity of 1C1-mcMMAF in EphA2-positive HeyA8-luc ovarian cancer cells at doses ranging from 1.0 to 5000 ng/mL by assessing cell survival. After incubation for 48 or 72 hours with 1C1-mcMMAF, cell survival was reduced in a dose-dependent manner compared with that of controls (1C1 or IgG-mcMMAF) (Figure 2, B). For example, after a 72-hour treatment with 1C1-mcMMAF at 100 ng/mL, reduced survival of HeyA8-luc cells (28.5%) was observed compared with that after treatment with 1C1 at 100 ng/mL (98.7%; difference = 70.2%, 95% CI = 66.3% to 74.0%; P < .001) or with IgG-mcMMAF at 100 ng/mL (99.6%; difference = 71.1%, 95% CI = 67.3% to 83.1%; P < .001). When apoptosis was assessed in cells stained with Annexin V–coupled FITC and propidium iodide by flow cytometry, statistically significantly more HeyA8-luc cells treated with 1C1-mcMMAF were apoptotic than those treated with the PBS control, 1C1, or IgG-mcMMAF (Figure 1, C and D and Supplementary Figure 1, available online). For example, the mean percentage of apoptotic cells after 72 hours of treatment with 1C1-mcMMAF was 30.1% compared with 4.9% after control treatment (difference = 25.2%, 95% CI = 24.8% to 25.5%; P < .001).

EphA2 Expression After Treatment of Ovarian Cancer Cell Lines or Tumors With 1C1-mcMMAF

Most ovarian cancer cell lines examined expressed medium to high levels of EphA2, as shown by Western blot analysis (Supplementary Figure 2, available online). Because anti-EphA2 antibodies can cause the internalization and degradation of EphA2, we investigated whether treatment with 1C1-mcMMAF would affect the levels of EphA2. In EphA2-positive HeyA8-luc cells, EphA2 expression was lower after treatment with 1C1 and 1C1-mcMMAF than after control treatment with PBS or IgG-mcMMAF for up to 48 hours, and by 72 hours, EphA2 expression had recovered to the levels in control cells (Figure 3, A). A similar pattern was observed in SKOV3ip1 cells (Supplementary Figure 3, available online).

For orthotopic ovarian tumors, we used the HeyA8-luc model and first examined EphA2 protein levels in tumors at 1–10 days after treatment with 1C1-mcMMAF by Western blot analysis and
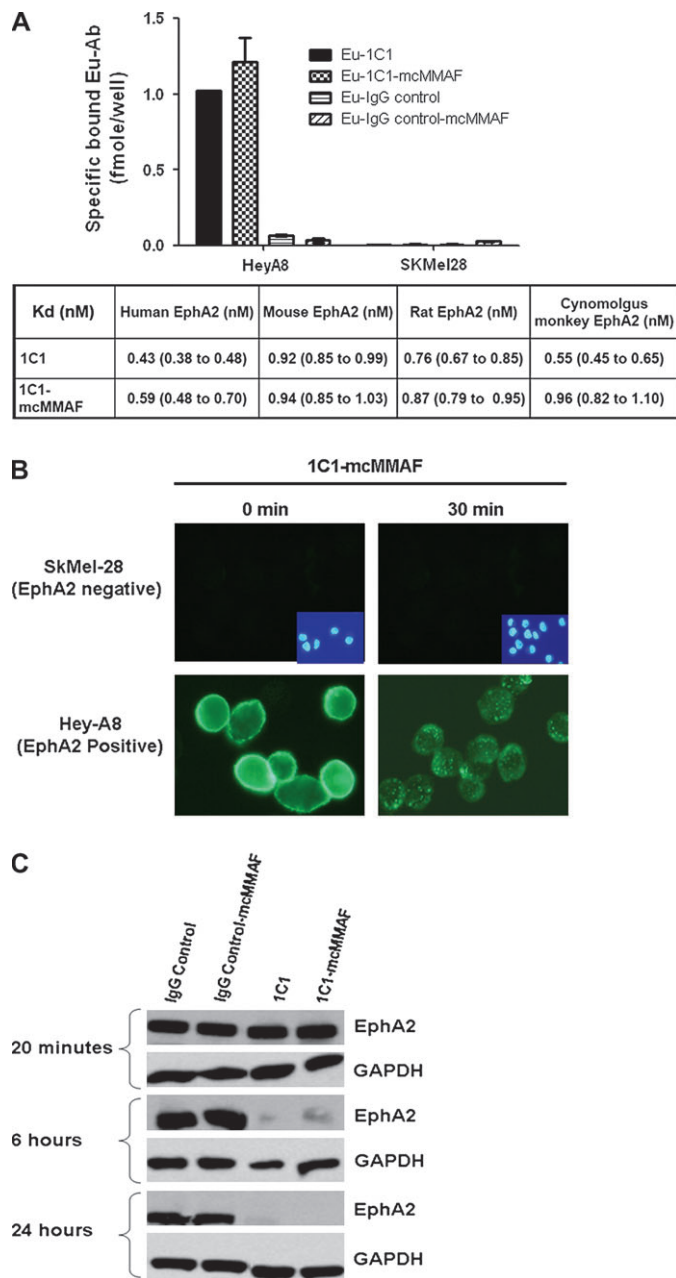
Figure 1. Characterization of anti-EphA2 immunoconjugates for receptor binding, internalization, and degradation. **A)** Binding activity of immunoconjugates. Binding activity of 1C1-mcMMAF (an immunoconjugate in which 1C1 is linked to a chemotherapeutic agent monomethyl auristatin phenylalanine [MMAF] by a noncleavable linker maleimidocaproyl [mc]), 1C1 (an anti-EphA2 monoclonal antibody), control IgG, and control IgG-mcMMAF was assessed by use of EphA2-expressing ovarian cell lines and recombinant EphA2 from various species. **Top)** Immunoconjugate binding activity to EphA2-expressing HeyA8 and EphA2-negative SKMel28 cells. Cell binding activity was assessed with a europium (Eu)-labeled antibody (Ab) binding assay. Eu-labeled antibodies and immunoconjugates examined were 1C1, 1C1-mcMMAF, an isotype control IgG, and control immunoconjugate IgG-mcMMAF. Error bars = 95% confidence intervals (CIs). **Bottom)** Comparison of the binding affinities (presented as dissociation constants [Kd] expressed in nanomolar) for 1C1 and 1C1-mcMMAF with recombinant EphA2 from various species. Data are the mean dissociation constants and 95% CIs. Experiments were preformed two times, with similar results in both experiments. **B)** Internalization of immunoconjugate by HeyA8 cells. Cells were immunostained for EphA2 with phosphate-buffered saline (PBS) containing the 1C1-mcMMAF or IgG-mcMMAF (each at 5 µg) and then incubated for 30 minutes at 4°C.

immunohistochemistry. Treatment with a single dose of 1C1-mcMMAF at 3 mg/kg reduced the expression of EphA2 protein in a time-dependent manner for up to 5 days. By day 10, EphA2 expression had recovered in at least one tumor (Figure 3, B and C). From this experiment, 1C1-mcMMAF dose of 3 mg/kg once a week was selected for subsequent experiments.

Treatment With 1C1-mcMMAF and Weight of Ovarian Carcinomas in Mice

To examine whether treatment of tumor-bearing mice with 1C1-mcMMAF affects tumor weight, we used three orthotopic models of ovarian cancer. Mice that were injected with either HeyA8-luc or SKOV3ip1 ovarian cancer cells were randomly assigned to one of the following four treatment groups (n = 10 mice per group), each receiving treatment once a week: PBS, 1C1, IgG-mcMMAF, or 1C1-mcMMAF (each at 3 mg/kg). After 3–5 weeks of therapy, the mice were killed by cervical dislocation and necropsy was performed. After 3 weeks of 1C1-mcMMAF treatment, the weight of HeyA8-luc tumors (0.05 g) was statistically significantly lower than the weight of tumors treated with PBS (1.03 g; difference = 0.98 g, 95% CI = 0.40 to 1.58 g; *P* = .001), 1C1 (0.67 g; difference = 0.62 g, 95% CI = 0.03 to 1.22 g; *P* = .037), or IgG-mcMMAF (0.85 g; difference = 0.81 g, 95% CI = 0.21 to 1.40 g; *P* = .006). After 5 weeks of 1C1-mcMMAF treatment, the weight of SKOV3ip1 tumors (0.10 g) was statistically significantly lower than the weight of tumors treated with PBS (0.65 g; difference = 0.55 g, 95% CI = 0.21 to 0.89 g; *P* = .001), 1C1 (0.42 g; difference = 0.32 g, 95% CI = 0.02 to 0.67 g; *P* = .045), or IgG-mcMMAF (0.54 g; difference = 0.44 g, 95% CI = 0.10 to 0.78 g; *P* = .008) (Figure 4, A and B). The route of immunoconjugate delivery (ie, intravenous vs intraperitoneal) was not associated with SKOV3ip1 tumor weight (Supplementary Figure 4, available online).

We also examined the taxane-resistant HeyA8-MDR tumor model because resistance to chemotherapy is common among patients with ovarian cancer. Mice injected with HeyA8-MDR cells were randomly assigned to one of the following four treatment groups (n = 10 mice per group): PBS, docetaxel at 50 µg per mouse once a week (15), 1C1 at 3 mg/kg once a week, or

Cells were then washed twice with PBS, and cell surface–bound immunoconjugates were allowed to internalize by resuspending the cells in 100 µL of growth medium (ie, RPMI 1640 medium and 10% fetal bovine serum) and incubation at 37°C in an atmosphere of 5% CO_2 and 95% air for 30 minutes or on ice as negative control (labeled 30 and 0 minutes, respectively). After this incubation, cells were fixed in 4% paraformaldehyde in 1× PBS for 20 minutes at room temperature and permeabilized in 0.5% Triton X-100 in 1× PBS for 5 minutes at room temperature. Cells were incubated with 1 µg of AlexaFluor 488-labeled goat anti-human IgG antibody (Biosource) in 100 µL of PBS containing 2% fetal bovine serum for 30 minutes at 4°C. **C)** Degradation of EphA2 receptors after immunoconjugate treatment. HeyA8 cells were treated with control IgG, control IgG-mcMMAF, 1C1, or 1C1-mcMMAF (each at 100 ng/mL) for 20 minutes, 6 hours, or 24 hours. Cell lysates were prepared and subjected to Western blot analysis with anti-EphA2 antibody to assess the total level of EphA2. Antibody binding was detected by incubating blots with horseradish peroxidase (HRP)–conjugated horse anti-mouse IgG or horse anti-rabbit IgG. HRP was visualized by use of an enhanced chemiluminescence detection kit. Experiments were preformed two times, with similar results in both experiments.
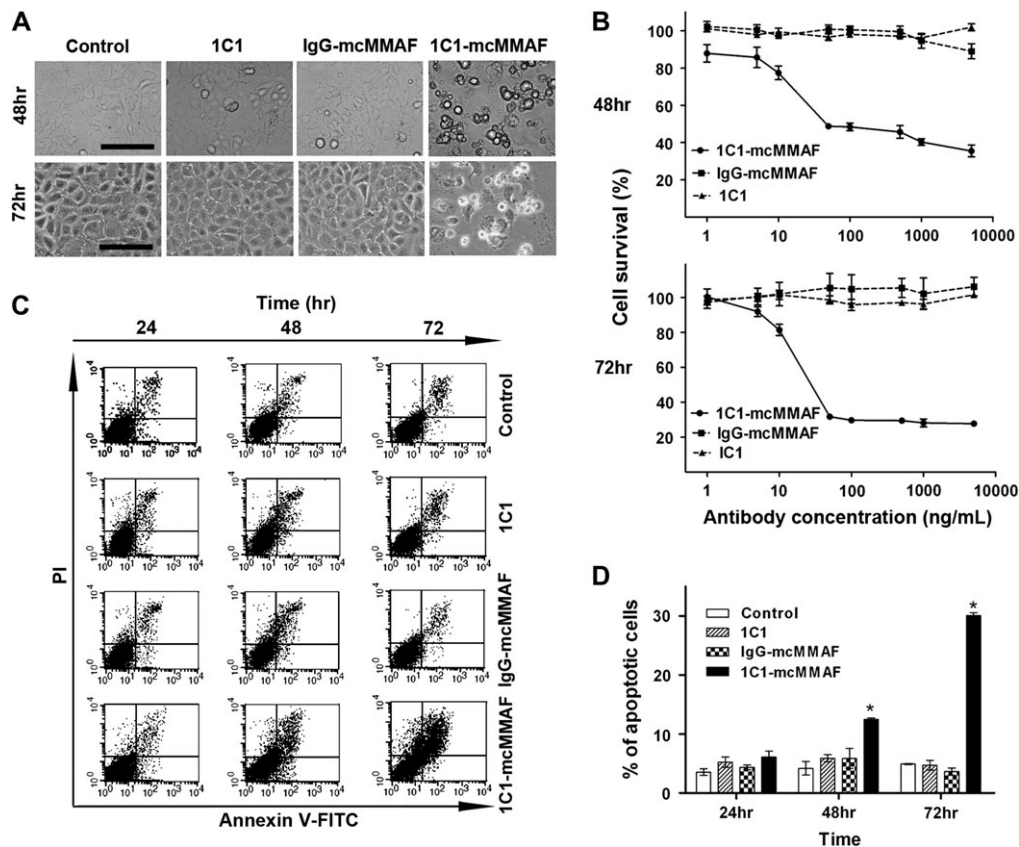
Figure 2. Cytotoxicity of immunoconjugate treatment. 1C1-mcMMAF is an immunoconjugate in which 1C1 (an anti-EphA2 monoclonal antibody) monoclonal antibody is linked to a chemotherapeutic agent monomethyl auristatin phenylalanine (MMAF) by a noncleavable linker maleimido-caproyl (mc). **A**) Apoptosis as assessed by cell morphology. EphA2-positive HeyA8-luc cells were incubated for 48 or 72 hours alone (control) or with 1C1, control immunoconjugate IgG-mcMMAF, or 1C1-mcMMAF (each at 100 ng/mL). Cell morphology was assessed by phase-contrast microscopy. Scale bar = 50 μm. **B**) Viability of cultured HeyA8-luc cells after immunoconjugate treatment. Viability was assessed with the 3-(4,5-dimethylthiazol-2-yl)-2,5-diphenyltetrazolium bromide assay at 48 and 72 hours after treatment with 1C1, control IgG-mcMMAF, or 1C1-mcMMAF (each at 1.0–5000 ng/mL). The experiment was performed three times, and each sample was repeated three times. Figure showed the data from one experiment, and the data of two others have similar results. Error bars = 95% confidence intervals (CIs). **C**) Apoptosis as detected by flow cytometry. HeyA8-luc cells were incubated alone (control) or with 1C1, IgG-mcMMAF, or 1C1-mcMMAF (each at 100 ng/mL) for 24–72 hours. Cells were stained with Annexin V coupled to fluorescein isothiocyanate (FITC) to identify apoptotic cells and propidium iodide (PI) to identify cell nuclei and then subjected to flow cytometry. In each panel, early apoptotic cells are shown in the upper right and late apoptotic cells are shown in the lower right. **D**) Percentage of apoptotic cells after immunoconjugate treatment. Data are from the flow cytometry experiment in (**C**). The percentage of cells that were positive for Annexin V staining was calculated. The experiment was repeated three times, with triplicates for each data point. Data are the mean. Error bars = 95% CIs. *$P < .001$, compared with control, 1C1, or IgG-mcMMAF. All statistical tests were two-sided.

1C1-mcMMAF at 3 mg/kg once a week. After 3 weeks of 1C1-mcMMAF treatment, the weight of HeyA8-MDR tumor was statistically significantly lower (0.42 g) than the weight of tumors treated with PBS (1.83 g; difference = 1.41 g, 95% CI = 0.36 to 2.46 g; $P = .006$) or docetaxel (1.33 g; difference = 0.91 g, 95% CI = 0.14 to 1.96 g; $P = .018$), but it was not statistically significantly lower than the weight of tumors treated with 1C1 (mean tumor weight = 1.07 g; difference = 0.65 g, 95% CI = 0.40 to 1.70 g; $P = .185$) (Figure 4, C).

We used body weight changes as an indication of cytotoxic side effects. No substantial difference in the body weight of mice across treatment groups (1C1, IgG-mcMMAF, or 1C1-mcMMAF immunoconjugate) was observed.

Although the models described above recapitulate disease patterns of patients with small ovarian tumors, many patients with ovarian cancer whose disease has relapsed have a larger tumor burden. Therefore, we also used in vivo bioluminescence imaging

to determine whether treatment with 1C1-mcMMAF could reduce the volume of larger tumors. Nude mice were intraperitoneally injected with HeyA8-luc cells, and 17 days later, treatment with 1C1-mcMMAF and bioluminescence imaging was initiated. Bioluminescence imaging was then performed at 3- to 4-day intervals thereafter. By day 21 after tumor cell injection, the volume of 1C1-mcMMAF–treated tumors had begun to decrease and continued to decrease through day 28 (Figure 5, A and B). Moreover, the 1C1-mcMMAF treatment (mean = 60.6 days) was associated with the higher survival than the control treatments with PBS (mean = 29.4 days; difference = 31.2 days, 95% CI = 27.6 to 31.2 days), 1C1 (mean = 29.8 days; difference = 30.8 days, 95% CI = 28.1 to 31.5 days), or IgG control-mcMMAF (mean = 30.8 days; difference = 29.8 days, 95% CI = 27.3 to 34.3 days). Survival in the 1C1-mcMMAF treatment group was statistically significantly different than that in the PBS, 1C1, or IgG-mcMMAF groups (each $P = .002$) (Figure 5, C).

1C1-mcMMAF Treatment and Cell Proliferation, Apoptosis, and Angiogenesis

To investigate potential mechanisms of 1C1-mcMMAF antitumor activity, we used the SKOV3ip1 tumor model to examine proliferation of tumor and endothelial cells. Proliferation was assessed by using PCNA staining. In tumors treated with 1C1-mcMMAF, 44.1% of nuclei were positive for PCNA compared with 55.8% in PBS-treated control tumors (difference = 11.7%, 95% CI = 2.45% to 20.9%; P = .01), 59.1% in 1C1-treated tumors (difference = 15%, 95% CI = 5.91% to 24.07%; P = .001), and 62.4% in control IgG-mcMMAF–treated tumors (difference = 18%, 95% CI = 9.17% to 27.33%; P < .001) (Figure 6, A). Similar patterns were observed in the HeyA8-luc and HeyA8-MDR tumor models (Supplementary Figure 5, A and B, available online).

Apoptosis was investigated by use of the TUNEL assay. Treatment with 1C1-mcMMAF also resulted in increased tumor cell apoptosis across all three mouse tumor models examined. For example, in SKOV3ip1 tumors treated with 1C1-mcMMAF, 8.6% of the tumor cells were positive for TUNEL compared with 0.9% in PBS-treated control tumors (difference = 7.7%, 95% CI = 3.8% to 11.7%; P < .001), 0.9% in 1C1-treated tumors (difference = 7.7%, 95% CI = 4.0% to 11.5%; P < .001), and 1.3% in control IgG-mcMMAF–treated tumors (difference = 7.3%, 95% CI = 3.6% to 11.1%; P < .001) (Supplementary Figures 5, A and B and 6, B, available online).

To determine if 1C1-mcMMAF treatment directly affected mouse ovarian endothelial cells (23), these cells were cultured and treated with 1C1-mcMMAF, 1C1, or IgG-mcMMAF for 48 or 72 hours and their survival was assessed by the MTT uptake assay. Survival of cells treated with 1C1-mcMMAF was lower than that of cells treated with 1C1 or IgG-mcMMAF (Supplementary Figure 6, A and B, available online). Because EphA2 is expressed on both tumor cells and endothelial cells in tumor angiogenic blood vessels, we also examined whether tumor vasculature was affected by treatment with 1C1-mcMMAF by assessing the viability of mouse endothelial cells in SKOV3ip1, HeyA8-luc, and HeyA8-MDR ovarian tumors. When we used TUNEL staining to identify apoptotic cells and CD31 staining to identify endothelial cells in tumors, tumors treated with 1C1-mcMMAF had more apoptotic endothelial cells (2.8%) than tumors treated with PBS (0.4%; difference = 2.4%, 95% CI = 0.1% to 4.6%; P = .034), 1C1 (0.4%; difference = 2.4%, 95% CI = 0.3% to 4.5%; P = .021), or IgG-mcMMAF (0.1%; difference = 2.7%, 95% CI = 0.6% to 4.8%; P = .007) (Figure 6, C) (Supplementary Figure 5, A [HeyA8-luc] and 5, B [HeyA8-MDR], available online). Thus, treatment of ovarian tumor–bearing mice with 1C1-mcMMAF appears to induce tumor regression by increasing the level of apoptosis in both tumor cells and endothelial cells.

Discussion

The key finding from this study is that EphA2-targeted chemotherapy appears to be a feasible and effective therapeutic approach for ovarian cancer. Delivery to ovarian cancer cells of MMAF conjugated with an EphA2-targeted monoclonal antibody via the noncleavable mc linker occurs in an EphA2-selective manner.
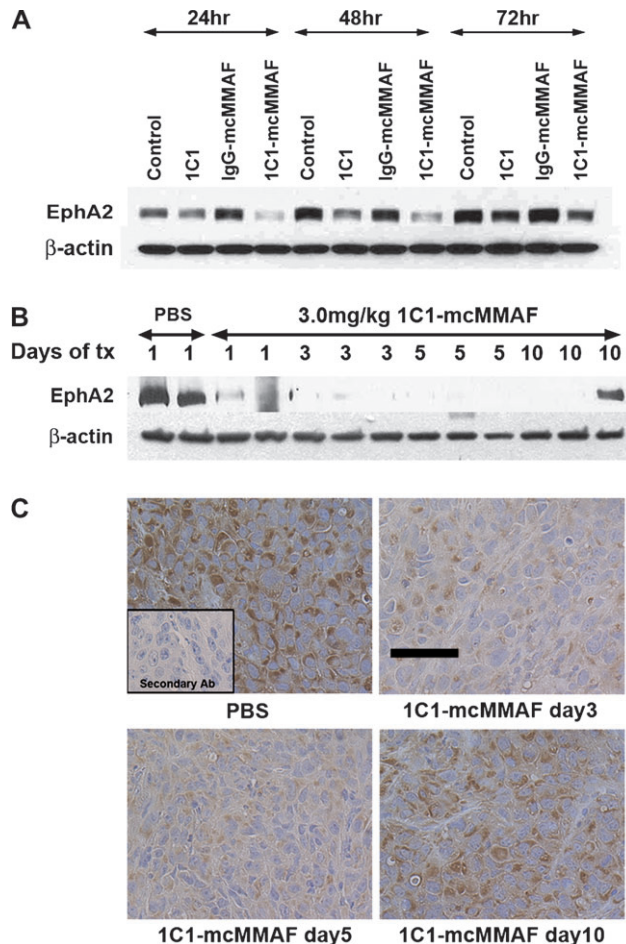

Figure 3. EphA2 expression after immunoconjugate treatment of HeyA8-luc cells or tumors. 1C1-mcMMAF is an immunoconjugate, in which 1C1 (an anti-EphA2 monoclonal antibody) is linked to the chemotherapeutic agent monomethyl auristatin phenylalanine (MMAF) by a noncleavable linker maleimidocaproyl (mc). **A**) EphA2 protein expression in cultured HeyA8-luc ovarian cancer cells after immunoconjugate treatment. Cells were treated with 1C1, control IgG-mcMMAF, or 1C1-mcMMAF (each at 100 ng/mL) for 24, 48, or 72 hours. Control at each time point represents the baseline expression of EphA2 at that point. Cell lysates were prepared and subjected to Western blot analysis with anti-EphA2 antibody to assess the total level of EphA2. Antibody binding was detected with horseradish peroxidase (HRP)–conjugated horse anti-mouse IgG or horse anti-rabbit IgG. HRP was visualized by use of an enhanced chemiluminescence detection kit. This experiment was repeated three times, each with similar results. **B**) EphA2 expression in HeyA8-luc tumors after immunoconjugate treatment. Mice were injected with HeyA8-luc cells and then 17 days later, when palpable intraperitoneal tumors were detected, were injected intraperitoneally once with 1C1-mcMMAF at 3 mg/kg or with phosphate-buffered saline (PBS) as control. Mice were killed at 1, 3, 5, or 10 days; tumors were collected; and tumor lysates were subjected to Western blot analysis for EphA2. Each lane contains tumor lysate from one mouse. Results were confirmed with a duplicate experiment. Tx = treatment. **C**) Immunohistochemistry of EphA2 expression in immunoconjugate-treated tumors. Tumor-bearing mice were treated with PBS (control) or with 1C1-mcMMAF at 3 mg/kg for 3, 5, or 10 days (n = 3) and then killed by cervical dislocation. Tumors were excised and sectioned. Sections were incubated with anti-EphA2 antibody, with biotinylated horse anti-mouse antibody, and then with streptavidin–HRP. Positive staining is shown by **brown** color. **Inset**) Negative control. Tissue section was incubated with only secondary antibody (Ab). This experiment was performed two times; results from both experiments were similar. Micrographs were taken at an original magnification of ×200. Scale bar = 50 µm.

Figure 4. Tumor weight after immunoconjugate treatment. 1C1-mcMMAF is an immunoconjugate, in which 1C1 (an anti-EphA2 monoclonal antibody) is linked to a chemotherapeutic agent monomethyl auristatin phenylalanine (MMAF) by a noncleavable linker maleimidocaproyl (mc). **A**) HeyA8-luc tumors. **B**) SKOV3ip1 tumors. **C**) Taxane-resistant HeyA8-MDR tumors. Mice were inoculated with HeyA8-luc, SKOV3ip1, or HeyA8-MDR cells and then 1 week later were treated with phosphate-buffered saline (PBS) (control) or with 1C1, IgG-mcMMAF, or 1C1-mcMMAF (each at 3 mg/kg). For HeyA8-MDR tumors, an additional group of mice were treated with docetaxel (50 µg per mouse, once a week). Mice in all groups were killed by cervical dislocation when control animals became moribund (3–5 weeks after initiating therapy, depending on the cell line used). All tumors were harvested; the tumor weight and number of tumor nodules were recorded. The tumors were located in the omentum, pelvis, peritoneum, mesentery, bowel wall, porta hepatis, diaphragm, or around the spleen. All of tumor nodules were analyzed (usually 1–25 nodules in HeyA8-luc, 1–26 nodules in SKOV3ip1, and 1–18 nodules in HeyA8-MDR model). Mean tumor weights with 95% confidence intervals and the weights of individual tumors are shown. Each treatment group contains 10 mice. There were 40 mice for each cell line. Statistical analysis for tumor weights was performed by two-sided Student t test (between two groups) and two-sided analysis of variance (multiple groups) because tumor weights were normally distributed (as determined by Kolmogrov–Smirnov test). All statistical tests were two-sided.
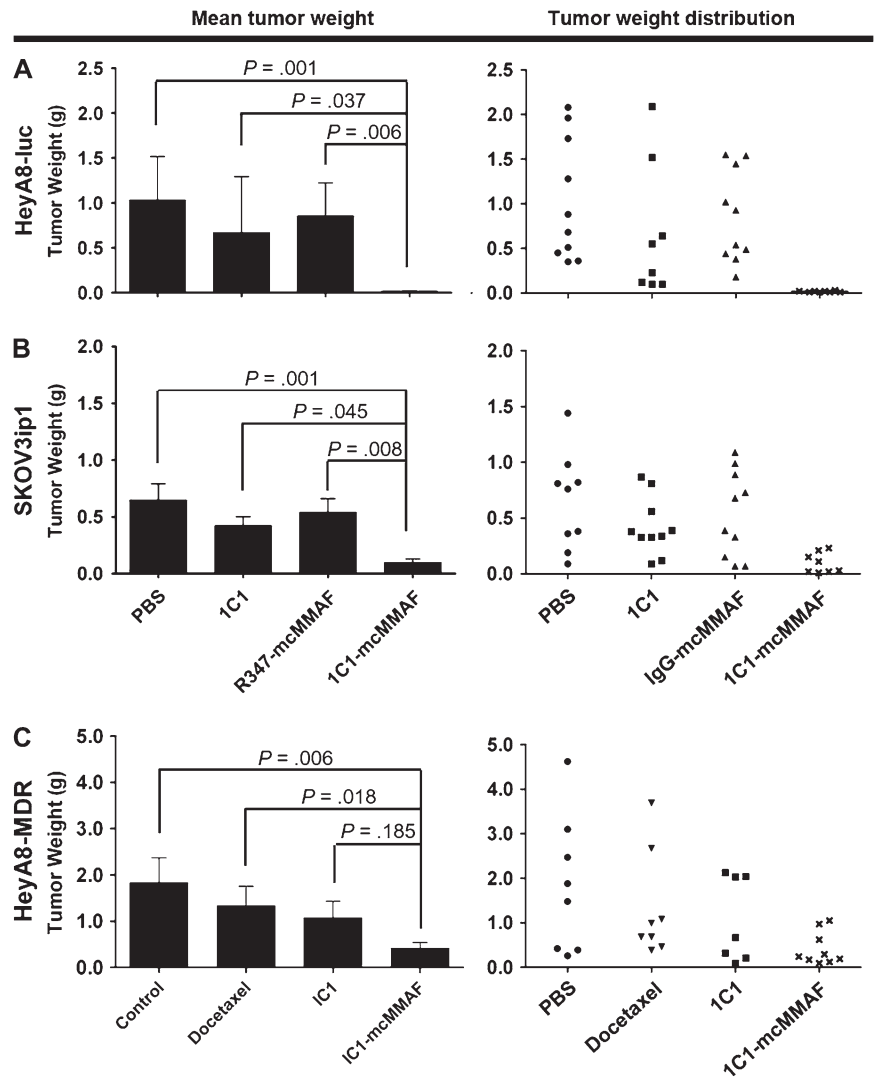
Moreover, this conjugate demonstrates therapeutic efficacy in models of small-volume and bulkier disease.

EphA2 is an attractive target for such an immunoconjugate approach because of its high expression in cancer tissues and its absence or low-level expression in epithelial tissues including kidney, lung, colon, and bladder (10). Landen et al. (8) reported that treatment with the EphA2 agonist antibody, EA5, resulted in moderate inhibition of tumor growth in orthotopic ovarian cancer models via regulation of angiogenesis factors. As expected, the 1C1 antibody did not demonstrate direct cytotoxicity in ovarian cancer or endothelial cells in vitro but allowed highly specific delivery of a cytotoxic payload (8).

In addition to the selection of a suitable chemotherapeutic agent and exploitation of a highly specific antibody, the linker chemistry is also important to ensure that the immunoconjugate is stable and can successfully deliver the drug to the target cell (24,25). Various linkers that are expected to be relatively stable outside the cells (in the blood) but to be labile inside cells have been designed. For example, dolastatins have been conjugated to CD30, CD70, or CD79 via peptide linkers containing valine–lysine sequence or β-glucuronic acid and found to be stable in blood but to be degraded in lysosomes, presumably by cathepsin B or β-glucuronidase (26–29).

To date, efforts to improve the cytotoxic actions of monoclonal antibodies and consequently their therapeutic effectiveness have focused on conjugates with highly toxic substances, including cytotoxic agents and radioisotopes (30–32). These conjugates can deliver a toxic payload selectively to the tumor site, while normal tissues are generally spared. Two radioimmunoconjugates including ibritumomab tiuxetan (Zevalin; Biogen Idec Inc, Cambridge, MA) and tositumomab (Bexxar; GlaxoSmithKline, Research Triangle Park, NC) have been approved in the United States for use in relapsed or refractory non-Hodgkin lymphoma (33,34). Both agents are murine monoclonal antibodies that target the CD20 antigen on B-cell lymphoma cells. An example of a cytotoxic agent conjugated to a monoclonal antibody is gemtuzumab ozogamicin (Mylotarg; Wyeth Pharmaceuticals Inc, Philadelphia, PA), which was approved in the United States in 2000 for treatment of acute myelogenous leukemia. This humanized IgG4 monoclonal antibody targets the CD33 antigen expressed on acute myelogenous leukemia blast cells and contains a calicheamicin γ1 derivative as the therapeutic agent that is

Figure 5. Immunoconjugate treatment of established ovarian carcinomas in mice. 1C1-mcMMAF is an immunoconjugate, in which 1C1 (an anti-EphA2 monoclonal antibody) is linked to a chemotherapeutic agent monomethyl auristatin phenylalanine (MMAF) by a noncleavable linker maleimidocaproyl (mc). **A**) Images of tumors in mice. Mice were injected intraperitoneally with HeyA8-luc cells and 17 days later were randomly assigned to treatment with PBS (control) or with 1C1, control IgG-mcMMAF, or 1C1-mcMMAF (each at 3 mg/kg). Bioluminescence imaging of each mouse was conducted at 3- to 4-day intervals. Data from days 17, 21, 24, 28, and 31 after cell injection are shown. The same mouse from each group is shown at each time point. The total number of mice was 20, and the number of mice per treatment group was five. **B**) Photon measurements from bioluminescence. Data are from the mice used in the experiment shown in (**A**). Signal intensity was quantified as the sum of all detected photons (p) within the region of interest per second (×10⁸). Error bars = 95% confidence intervals for the means. **C**) Survival of HeyA8-luc tumor-bearing mice after treatment. Mice used in bioluminescence experiment in (**A**) were used for the survival analysis. Survival was analyzed by the Kaplan–Meier method ($P = .001$). Mice treated with 1C1-mcMMAF (mean = 60.6 days) had the longest survival compared with those treated with PBS control (mean = 29.4 days; difference = 31.2 days, 95% CI = 27.6 to 31.2), 1C1 (mean = 29.8 days; difference = 30.8 days, 95% CI = 28.1 to 31.5 days), or IgG-mcMMAF (mean = 30.8 days; difference = 29.8 days, 95% CI = 27.3 to 34.3 days) (each $P = .002$).
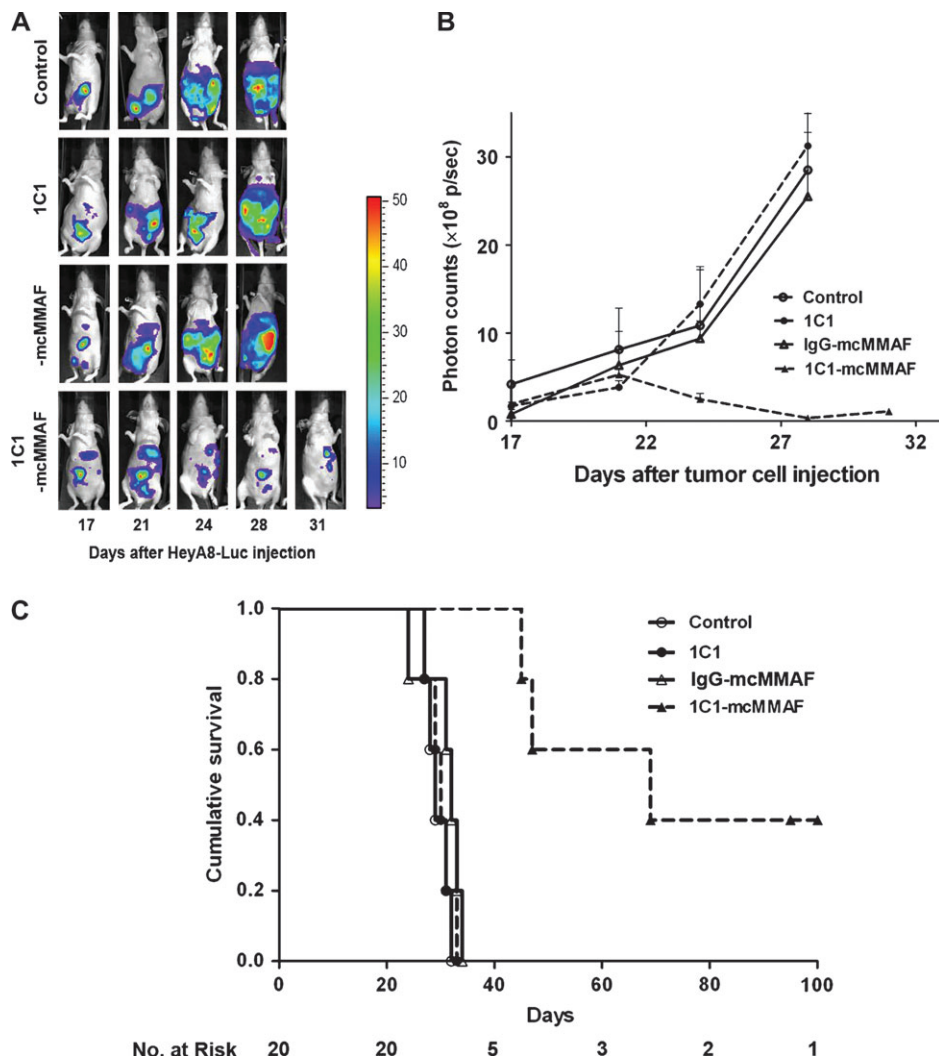
attached via a bifunctional linker (35). Other conjugates of monoclonal antibodies with cytotoxic toxins are under clinical evaluation (36). Immunoconjugates that contain auristatins induce cell cycle arrest at the G_2–M border, microtubule disruption, and apoptosis induction. Several immunoconjugates containing auristatin analogs targeted to cell surface markers such as CD20, CD30, and prostate specific membrane antigen have already shown promise in preclinical and clinical studies (12,24,26,37–43).

Work with tumor-based models suggests potential roles for EphA2 in the regulation of cell growth, survival, migration, and angiogenesis (44–48). EphA2 expression is frequently elevated in breast (49–51), colon (45), prostate (52), and non–small cell lung cancers (53), and aggressive melanomas (54). Whereas the expression of EphA2 receptor in human cancer has been well established, little is known about its role in normal adult tissues. The expression of EphA2 mRNA and protein has been described in adult rat kidney and lung epithelial cells (9). Similar analysis has detected EphA2 mRNA in adult human tissues of the kidney and lung, as well as in colon and bladder (55). However, imaging studies using a radiolabeled version of the highly selective antibody

1C1 revealed preferential distribution to tumors with no accumulation in any normal mouse or rat tissues (56), suggesting that targeting of the immunoconjugate to normal mouse tissues is minimal.

Our study had several potential limitations. First, although we found that 1C1-mcMMAF could decrease the tumor volume in bulkier tumor model with HeyA8-luc-luc, we have not evaluated the actual delivery of this immunoconjugate into the solid tumor mass. Second, in spite of the safety of 1C1-mcMMAF in preclinical experiments, unexpected toxicities may be identified in future research, especially to EphA2-expressing normal tissues or cells. Further preclinical safety evaluation will be needed before clinical development. Third, analyses in this report were done in cultured cell lines and in mouse models that used immunodeficient mice, and so results may not necessarily translate into human patients with ovarian cancer.

In summary, the findings herein provide a novel EphA2-targeted immunoconjugate with potent antitumor activity in ovarian carcinoma. Further preclinical and clinical development of the 1C1-mcMMAF immunoconjugate appears to be warranted.
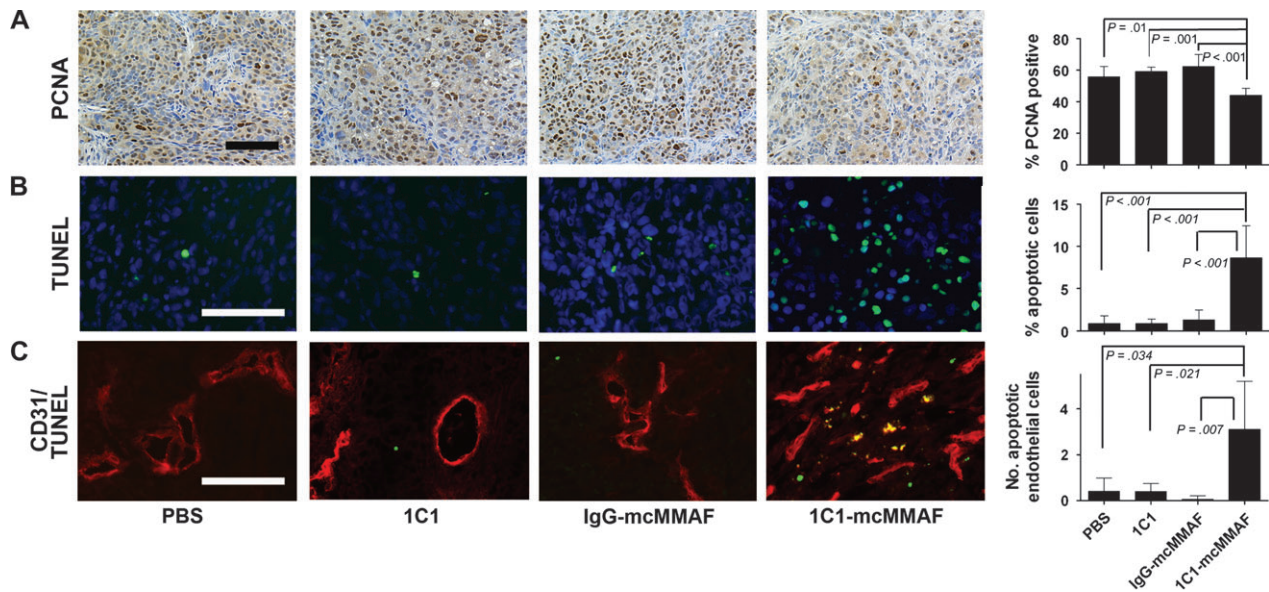
Figure 6. Proliferation and apoptosis of tumor or endothelial cells in SKOV3ip1 tumors after immunoconjugate treatment. 1C1-mcMMAF is an immunoconjugate, in which 1C1 (an anti-EphA2 monoclonal antibody) is linked to a chemotherapeutic agent monomethyl auristatin phenylalanine (MMAF) by a noncleavable linker maleimidocaproyl (mc). Mice bearing SKOV3ip1 ovarian tumors were treated with phosphate-buffered saline (PBS), 1C1, control IgG-mcMMAF, or 1C1-mcMMAF. When control mice became moribund, all mice in that treatment group were killed by cervical dislocation. Tumors were fixed in formalin and embedded in paraffin or were snap-frozen in optimal cutting temperature compound in liquid nitrogen. **A**) Tumor cell proliferation as assessed by proliferating cell nuclear antigen (PCNA). PCNA was detected with antibody against PNCA followed by horseradish peroxidase–conjugated secondary antibody and visualized with diaminobenzidine as the substrate (**brown**). PCNA-positive cells were counted, and the percentage of total cells was plotted in the histogram at the right. Five samples were used from each group, and results were confirmed with a duplicate experiment. Error bars = 95% confidence intervals. **B**) Apoptosis as assessed by deoxynucleotidyltransferase-mediated nick end labeling (TUNEL). Tumor sections were stained with both oechst (**blue**) to identify nuclei and TUNEL (**green**) to identify apoptotic cells and viewed under double immunofluorescence microscopy. Apoptotic cells were counted, and the percentage of total cells was plotted in the histogram at the right. **C**) Apoptosis in mouse endothelial cells in the SKOV3ip1 tumors after treatment. Tumor sections were stained with CD31 (**red**) to identify mouse endothelial cells and TUNEL (**green**) to identify apoptotic cells and visualized under double immunofluorescence microscopy. Endothelial cells undergoing apoptosis appear **yellow**. Original magnifications: (**A**) = ×100; (**B**) and (**C**) = ×200. Black scale bar = 100 µm; white scale bar = 50 µm.

References

1. Jemal A, Siegel R, Ward E, et al. Cancer statistics, 2006. *CA Cancer J Clin.* 2006;56(2):106–130.
2. Lister-Sharp D, McDonagh MS, Khan KS, Kleijnen J. A rapid and systematic review of the effectiveness and cost-effectiveness of the taxanes used in the treatment of advanced breast and ovarian cancer. *Health Technol Assess.* 2000;4(17):1–113.
3. Baek S-J, Park J-Y, Kim D-Y, et al. Stage IIIC epithelial ovarian cancer classified solely by lymph node metastasis has a more favorable prognosis than other types of stage IIIC epithelial ovarian cancer. *J Gynecol Oncol.* 2008;19(4):223–228.
4. Partridge EE, Barnes MN. Epithelial ovarian cancer: prevention, diagnosis, and treatment. *CA Cancer J Clin.* 1999;49(5):297–320.
5. Zangemeister-Wittke U. Antibodies for targeted cancer therapy—technical aspects and clinical perspectives. *Pathobiology.* 2005;72(6):279–286.
6. Ricart AD, Tolcher AW. Technology insight: cytotoxic drug immunoconjugates for cancer therapy. *Nat Clin Pract Oncol.* 2007;4(4):245–255.
7. Lin YG, Han LY, Kamat AA, et al. EphA2 overexpression is associated with angiogenesis in ovarian cancer. *Cancer.* 2007;109(2):332–340.
8. Landen CN Jr, Lu C, Han LY, et al. Efficacy and antivascular effects of EphA2 reduction with an agonistic antibody in ovarian cancer. *J Natl Cancer Inst.* 2006;98(21):1558–1570.
9. Lindberg RA, Hunter T. cDNA cloning and characterization of eck, an epithelial cell receptor protein-tyrosine kinase in the eph/elk family of protein kinases. *Mol Cell Biol.* 1990;10(12):6316–6324.
10. Walker-Daniels J, Hess AR, Hendrix MJ, Kinch MS. Differential regulation of EphA2 in normal and malignant cells. *Am J Pathol.* 2003;162(4):1037–1042.
11. Jackson D, Gooya J, Mao S, et al. A human antibody-drug conjugate targeting EphA2 inhibits tumor growth in vivo. *Cancer Res.* 2008;68(22):9367–9374.
12. Doronina SO, Toki BE, Torgov MY, et al. Development of potent monoclonal antibody auristatin conjugates for cancer therapy. *Nat Biotechnol.* 2003;21(7):778–784.
13. Doronina SO, Bovee TD, Meyer DW, et al. Novel peptide linkers for highly potent antibody-auristatin conjugate. *Bioconjug Chem.* 2008;19(10):1960–1963.
14. Lu C, Kamat AA, Lin YG, et al. Dual targeting of endothelial cells and pericytes in antivascular therapy for ovarian carcinoma. *Clin Cancer Res.* 2007;13(14):4209–4217.
15. Halder J, Kamat AA, Landen CN Jr, et al. Focal adhesion kinase targeting using in vivo short interfering RNA delivery in neutral liposomes for ovarian carcinoma therapy. *Clin Cancer Res.* 2006;12(16):4916–4924.
16. Merritt WM, Lin YG, Spannuth WA, et al. Effect of interleukin-8 gene silencing with liposome-encapsulated small interfering RNA on ovarian cancer cell growth. *J Natl Cancer Inst.* 2008;100(5):359–372.
17. Kamat AA, Kim TJ, Landen CN Jr, et al. Metronomic chemotherapy enhances the efficacy of antivascular therapy in ovarian cancer. *Cancer Res.* 2007;67(1):281–288.
18. Merritt WM, Lin YG, Han LY, et al. Dicer, Drosha, and outcomes in patients with ovarian cancer. *N Engl J Med.* 2008;359(25):2641–2650.
19. Shishodia S, Majumdar S, Banerjee S, Aggarwal BB. Ursolic acid inhibits nuclear factor-kappaB activation induced by carcinogenic agents through suppression of IkappaBalpha kinase and p65 phosphorylation: correlation with down-regulation of cyclooxygenase 2, matrix metalloproteinase 9, and cyclin D1. *Cancer Res.* 2003;63(15):4375–4383.

20. Landen CN, Kinch MS, Sood AK. EphA2 as a target for ovarian cancer therapy. *Expert Opin Ther Targets*. 2005;9(6):1179–1187.

21. Apte SM, Fan D, Killion JJ, Fidler IJ. Targeting the platelet-derived growth factor receptor in antivascular therapy for human ovarian carcinoma. *Clin Cancer Res*. 2004;10(3):897–908.

22. Baker CH, Kedar D, McCarty MF, et al. Blockade of epidermal growth factor receptor signaling on tumor cells and tumor-associated endothelial cells for therapy of human carcinomas. *Am J Pathol*. 2002;161(3):929–938.

23. Langley RR, Ramirez KM, Tsan RZ, Van Arsdall M, Nilsson MB, Fidler IJ. Tissue-specific microvascular endothelial cell lines from H-2K(b)-tsA58 mice for studies of angiogenesis and metastasis. *Cancer Res*. 2003;63(11):2971–2976.

24. Doronina SO, Mendelsohn BA, Bovee TD, et al. Enhanced activity of monomethylauristatin F through monoclonal antibody delivery: effects of linker technology on efficacy and toxicity. *Bioconjug Chem*. 2006;17(1):114–124.

25. Schrama D, Reisfeld RA, Becker JC. Antibody targeted drugs as cancer therapeutics. *Nat Rev Drug Discov*. 2006;5(2):147–159.

26. Sutherland MS, Sanderson RJ, Gordon KA, et al. Lysosomal trafficking and cysteine protease metabolism confer target-specific cytotoxicity by peptide-linked anti-CD30-auristatin conjugates. *J Biol Chem*. 2006;281(15):10540–10547.

27. Jeffrey SC, Torgov MY, Andreyka JB, et al. Design, synthesis, and in vitro evaluation of dipeptide-based antibody minor groove binder conjugates. *J Med Chem*. 2005;48(5):1344–1358.

28. Jeffrey SC, Andreyka JB, Bernhardt SX, et al. Development and properties of beta-glucuronide linkers for monoclonal antibody-drug conjugates. *Bioconjug Chem*. 2006;17(3):831–840.

29. Jeffrey SC, Nguyen MT, Andreyka JB, Meyer DL, Doronina SO, Senter PD. Dipeptide-based highly potent doxorubicin antibody conjugates. *Bioorg Med Chem Lett*. 2006;16(2):358–362.

30. Sharkey RM, Goldenberg DM. Targeted therapy of cancer: new prospects for antibodies and immunoconjugates. *CA Cancer J Clin*. 2006;56(4):226–243.

31. Reff ME, Heard C. A review of modifications to recombinant antibodies: attempt to increase efficacy in oncology applications. *Crit Rev Oncol Hematol*. 2001;40(1):25–35.

32. Wu AM, Senter PD. Arming antibodies: prospects and challenges for immunoconjugates. *Nat Biotechnol*. 2005;23(9):1137–1146.

33. Nowakowski GS, Witzig TE. Radioimmunotherapy for B-cell non-Hodgkin lymphoma. *Clin Adv Hematol Oncol*. 2006;4(3):225–231.

34. Cheson BD. Radioimmunotherapy of non-Hodgkin lymphomas. *Blood*. 2003;101(2):391–398.

35. van Der Velden VH, te Marvelde JG, Hoogeveen PG, et al. Targeting of the CD33-calicheamicin immunoconjugate Mylotarg (CMA-676) in acute myeloid leukemia: in vivo and in vitro saturation and internalization by leukemic and normal myeloid cells. *Blood*. 2001;97(10):3197–3204.

36. Chen J, Jaracz S, Zhao X, Chen S, Ojima I. Antibody-cytotoxic agent conjugates for cancer therapy. *Expert Opin Drug Deliv*. 2005;2(5):873–890.

37. Law CL, Gordon KA, Toki BE, et al. Lymphocyte activation antigen CD70 expressed by renal cell carcinoma is a potential therapeutic target for anti-CD70 antibody-drug conjugates. *Cancer Res*. 2006;66(4):2328–2337.

38. Francisco JA, Cerveny CG, Meyer DL, et al. cAC10-vcMMAE, an anti-CD30-monomethyl auristatin E conjugate with potent and selective antitumor activity. *Blood*. 2003;102(4):1458–1465.

39. Law CL, Cerveny CG, Gordon KA, et al. Efficient elimination of B-lineage lymphomas by anti-CD20-auristatin conjugates. *Clin Cancer Res*. 2004;10(23):7842–7851.

40. Smith LM, Nesterova A, Alley SC, Torgov MY, Carter PJ. Potent cytotoxicity of an auristatin-containing antibody-drug conjugate targeting melanoma cells expressing melanotransferrin/p97. *Mol Cancer Ther*. 2006;5(6):1474–1482.

41. Tse KF, Jeffers M, Pollack VA, et al. CR011, a fully human monoclonal antibody-auristatin E conjugate, for the treatment of melanoma. *Clin Cancer Res*. 2006;12(4):1373–1382.

42. Afar DE, Bhaskar V, Ibsen E, et al. Preclinical validation of anti-TM-EFF2-auristatin E-conjugated antibodies in the treatment of prostate cancer. *Mol Cancer Ther*. 2004;3(8):921–932.

43. Bhaskar V, Law DA, Ibsen E, et al. E-selectin up-regulation allows for targeted drug delivery in prostate cancer. *Cancer Res*. 2003;63(19):6387–6394.

44. Andres AC, Reid HH, Zurcher G, Blaschke RJ, Albrecht D, Ziemiecki A. Expression of two novel eph-related receptor protein tyrosine kinases in mammary gland development and carcinogenesis. *Oncogene*. 1994;9(5):1461–1467.

45. Rosenberg IM, Goke M, Kanai M, Reinecker HC, Podolsky DK. Epithelial cell kinase-B61: an autocrine loop modulating intestinal epithelial migration and barrier function. *Am J Physiol*. 1997;273(4, pt 1):G824–G832.

46. Pandey A, Shao H, Marks RM, Polverini PJ, Dixit VM. Role of B61, the ligand for the Eck receptor tyrosine kinase, in TNF-alpha-induced angiogenesis. *Science*. 1995;268(5210):567–569.

47. Pandey A, Lazar DF, Saltiel AR, Dixit VM. Activation of the Eck receptor protein tyrosine kinase stimulates phosphatidylinositol 3-kinase activity. *J Biol Chem*. 1994;269(48):30154–30157.

48. Ganju P, Shigemoto K, Brennan J, Entwistle A, Reith AD. The Eck receptor tyrosine kinase is implicated in pattern formation during gastrulation, hindbrain segmentation and limb development. *Oncogene*. 1994;9(6):1613–1624.

49. Zantek ND, Azimi M, Fedor-Chaiken M, Wang B, Brackenbury R, Kinch MS. E-cadherin regulates the function of the EphA2 receptor tyrosine kinase. *Cell Growth Differ*. 1999;10(9):629–638.

50. Zelinski DP, Zantek ND, Stewart JC, Irizarry AR, Kinch MS. EphA2 overexpression causes tumorigenesis of mammary epithelial cells. *Cancer Res*. 2001;61(5):2301–2306.

51. Zantek ND, Walker-Daniels J, Stewart J, et al. MCF-10A-NeoST: a new cell system for studying cell-ECM and cell-cell interactions in breast cancer. *Clin Cancer Res*. 2001;7(11):3640–3648.

52. Walker-Daniels J, Coffman K, Azimi M, et al. Overexpression of the EphA2 tyrosine kinase in prostate cancer. *Prostate*. 1999;41(4):275–280.

53. D'Amico TA, Aloia TA, Moore MB, et al. Predicting the sites of metastases from lung cancer using molecular biologic markers. *Ann Thorac Surg*. 2001;72(4):1144–1148.

54. Easty DJ, Bennett DC. Protein tyrosine kinases in malignant melanoma. *Melanoma Res*. 2000;10(5):401–411.

55. Hafner C, Schmitz G, Meyer S, et al. Differential gene expression of Eph receptors and ephrins in benign human tissues and cancers. *Clin Chem*. 2004;50(3):490–499.

56. Cai W, Ebrahimnejad A, Chen K, et al. Quantitative radioimmunoPET imaging of EphA2 in tumor-bearing mice. *Eur J Nucl Med Mol Imaging*. 2007;34(12):2024–2036.

Funding

Notes